HHS Public Access

Author manuscript

Osteoarthritis Cartilage. Author manuscript; available in PMC 2017 April 01.

Published in final edited form as:

Osteoarthritis Cartilage. 2016 April ; 24(4): 752–762. doi:10.1016/j.joca.2015.10.016.

Acid Ceramidase Treatment Enhances the Outcome of Autologous Chondrocyte Implantation in a Rat Osteochondral Defect Model

Michael E. Frohbergh, PhD[1], **Johana M. Guevara, PhD**[2], **Ronald P. Grelsamer, MD**[3], **Mary F. Barbe, PhD**[4], **Xingxuan He, MD**[1], **Calogera M. Simonaro, PhD**[1], and **Edward H. Schuchman, PhD**[1,*]

[1]Department of Genetics and Genomic Science, Icahn School of Medicine at Mount Sinai, New York, NY

[2]Institute for the Study of Inborn Errors of Metabolism, Pontificia Universidad Javeriana, Bogota, Colombia

[3]Department of Orthopedic Surgery, Icahn School of Medicine at Mount Sinai, New York, NY

[4]Department of Anatomy and Cell Biology, Temple University, Philadelphia, PA

Abstract

Objective—The overall aim of this study was to evaluate how supplementation of chondrocyte media with recombinant acid ceramidase (rhAC) influenced cartilage repair in a rat osteochondral defect model.

Methods—Primary chondrocytes were grown as monolayers in polystyrene culture dishes with and without rhAC (added once at the time of cell plating) for 7 days, and then seeded onto Bio-Gide® collagen scaffolds and grown for an additional 3 days. The scaffolds were then introduced into osteochondroal defects created in Sprague-Dawley rat trochlea by a micordrilling procedure.

*Corresponding Author: Edward H. Schuchman, PhD, Department of Genetics and Genomic Science, Icahn School of Medicine at Mount Sinai, 1425 Madison Avenue, Rm. 14-20A, New York, NY 10029, Tel: 212-659-6711; Fax: 212-849-2447, Edward.schuchman@mssm.edu.

Author contributions

Michael E. Frohbergh contributed to the design, acquisition of data, analysis, interpretation, drafting and revising of this manuscript until final approval.

Johana Guevara contributed to the analysis and interpretation of the data and drafting and revising of this manuscript until final approval.

Mary F. Barbe contributed to the design, acquisition and interpretation of the microCT data at Temple University until final approval.

Ron P. Grelsamer contributed to the design and employment of osteochondral defect surgery in the rat model throughout the course of this study, as well as drafting and revising the manuscript until final approval.

Calogera M. Simonaro contributed to the overall design, analysis, interpretation, drafting and revision of this manuscript until final approval.

Edward H. Schuchman contributed the overall design, analysis, interpretation, drafting and revision of this manuscript until final approval.

Conflict of interest

All other authors have no conflict of interest.

Analysis was performed 6 weeks post-surgery macroscopically, by micro-CT, histologically, and by immunohistochemistry.

Results—Treatment with rhAC led to increased cell numbers and glycosaminoglycan production (~2 and 3-fold, respectively) following 7 days of expansion *in vitro*. Gene expression of collagen 2, aggrecan and Sox-9 also was significantly elevated. After seeding onto Bio-Gide®, more rhAC treated cells were evident within 4 hours. At 6 weeks post-surgery, defects containing rhAC-treated cells exhibited more soft tissue formation at the articular surface, as evidenced by microCT, as well as histological evidence of enhanced cartilage repair. Notably, collagen 2 immunostaining revealed greater surface expression in animals receiving rhAC treated cells as well. Collagen 10 staining was not enhanced.

Conclusion—The results further demonstrate the positive effects of rhAC treatment on chondrocyte growth and phenotype *in vitro*, and reveal for the first time the *in vivo* effects of the treated cells on cartilage repair.

Keywords

Acid Ceramidase; Autologous Chondrocyte Implantation; Osteochondral Defect Model; Primary Chondrocyte Expansion; Cartilage Tissue Engineering; In Vivo

Introduction

Articular cartilage diseases affect over 25 million adults a year in the United States [1]. Current surgical treatments consist of joint replacement, osteotomies, micro-fracture, autologous chondrocyte implantation (ACI), and/or allografts and autografts. ACI uses a biopsy of healthy knee cartilage to isolate chondrocytes, which are then expanded *in vitro* and injected into the site of injury [2]. Despite the increasing popularity of ACI, there remain a number of unresolved issues [3–5], that limits its effectiveness.

To overcome these obstacles many investigators have focused on the re-differentiation and maintenance of expanded chondrocytes [3–6]. In our lab we have previously reported the effects of exogenous recombinant human acid ceramidase (rhAC) on the de-differentiation of chondrocytes by observing specific chondrocyte markers at the protein level, and also showed that this enzyme treatment enhanced survival of the expanded cells [7].

Acid ceramidase (AC) is an enzyme responsible for the hydrolysis of ceramides to sphingosine and fatty acids, which is further phosphorylated to produce sphingosine-1-phosphate (S1P) [8, 9]. Each of these lipids is highly bioactive and has important roles in cell signaling and survival [9–13]. AC's importance in mammalian development is highlighted by the fact that knockout mice die by the 4-cell stage of embryogenesis [14, 15]. In addition, patients with inherited AC mutations present with Farber Lipogranulomatosis, characterized by severe juvenile arthritis and early death [8, 14, 16–18].

In this study a rodent model was employed to test the efficacy and wound healing capabilities of rhAC treated chondrocytes. Rodents are a common proof-of-concept model used to observe articular cartilage therapies prior to larger animal models and human trials [19–22]. The overall goal of this study was to continue to evaluate the effects of rhAC

treatment on articular chondrocytes, and to use a rat osteochondral defect model to determine if this treatment provided a better quality repair *in vivo*.

Materials and Methods

Animals

Animals were raised and cared for under NIH and USDA guidelines. All protocols were approved by the Mount Sinai Institutional Animal Care and Use Committee (Protocol # LA13-00002). Housing was in specific pathogen-free (SPF) rooms maintained with sentinels and *ad libitum* food and water. Euthanasia procedures were performed in accordance with the American Veterinary Medical Association guidelines.

Cell Isolation, Culture and Expansion

Chondrocytes were isolated from the articular surfaces of healthy 6-month old (~500g) female Sprague-Dawley rats (Charles River Laboratories, Wilmington, MA). Two rats were used per isolation, and cells were pooled to obtain enough for proper culture and expansion. Cells were isolated according to previously reported methods [7]. Briefly, animals were euthanized using CO_2 and the meniscus from each knee joint was removed along with scraping of the articular surface. The tissue isolates were collected in fresh DMEM containing 10% FBS (v/v), 1% penicillin/streptomycin (v/v), 1% L-glutamine (v/v) and 0.1% fungizone (v/v), minced with scissors, and then transferred to DMEM containing 1mg/mL protease from *Streptomyces griseus* and rotated at 37°C for 2 hours. They were then incubated in DMEM containing 1mg/mL collagenase type II and rotated at 37°C overnight. The remaining tissue was strained three times through 40μm nylon mesh filters to remove debris. The cell suspension was centrifuged (1000rpm for 5 minutes) and cells were plated at a density of 10,000 cells/cm^2 and cultured in complete DMEM in tissue culture polystyrene (TCP) flasks. On average, ~250,000 cells were collected per isolation. Media was changed every 3 days. Cells were grown with and without rhAC (12.5μg/mL) supplemented culture medium. rhAC is a recombinant enzyme produced from Chinese hamster ovary (CHO cells) as previously described [23]. It was only added on day 1, when the cells were first plated. Cells were expanded to ~90% confluence (7 days) and cell numbers were recorded using a hemocytometer.

RT-qPCR and Glycosaminoglycan (GAG) Content

After 7 days of expansion, chondrocytes were harvested from the culture flasks by trypsinization and collected as cell pellets (~1×10^6 cells/pellet). RNA was extracted using the qiaShredder and RNeasy Mini Kit (Qiagen, Limburg, Netherlands) and quantified using the Nanodrop 1000 (Thermo Scientific, Walthman, MA). Complementary DNA was synthesized using the high capacity cDNA reverse transcription kit (Life Technologies, Grand Island, NY) and a Bio-Rad S1000 thermal cycler (Bio-Rad, Hercules, CA). RT-qPCR used the fast universal PCR Master Mix and primers (Life Technologies, Grand Island, NY) specific for collagen II (Col2a1, Rn01637087_m1), aggrecan (Agg, Rn00573424_m1), Sox9 (Sox9, Rn01751069_mH), collagen X (Col10a1, Rn01408030_m1) and GAPDH (Rn01775763_g1 as a housekeeping gene), and ran on a 7900HT qPCR machine (Life

Technologies, Grand Island, NY). The ΔΔct method was used to analyze the data and the results were presented as relative quantity (RQ) fold change.

GAG content was measured on the cell pellets using the Blyscan (BioColor, United Kingdom) sulfated GAG assay kit, a dimethymethylene blue binding assay, according to the manufacturer's instructions. Absorbance of the final solution was observed at 656nm on a Synergy HT microplate reader (BioTek, Winooski, VT).

Scaffold Preparation and Cell Seeding

Bio-Gide® (Geistlich, Germany) sheets were provided by the Department of Orthopedic Surgery at the Icahn School of Medicine at Mount Sinai. Ten mm diameter circles were prepared and fitting into 48 well plates with Viton® O-rings (Dupont, Wilmington, DE). The scaffolds were exposed to UV light for 30 minutes on each side for sterilization and pre-treated in complete DMEM overnight at 37°C and 5% CO_2 incubation. Expanded (7 day) chondrocytes were trypsinized at 90% confluency and seeded directly onto the surface of the pre-treated Bio-Gide® at a density of 5×10^4 cells/scaffold. The scaffolds were seeded 3 days prior to implantation to allow for appropriate cell attachment. Cells were quantified at 4 and 72 hours to observe rhAC effects on adhesion and proliferation by staining with DAPI nuclear stain (Life Technologies, Grand Island, NY) and counting four relative grids from each scaffold for an estimated total cell number on the scaffold. For implantation, 2mm diameter samples were removed from the seeded scaffolds using a punch biopsy (Sklar Instruments, West Chester, PA).

Surgical Procedure

Six-month-old (~500g) female Sprague-Dawley rats were anesthetized using ketamine/xylazine (80mg/kg and 5mg/kg, respectively) administered by intraperitoneal (IP) injection in an IACUC approved animal laboratory facility. A subcutaneous injection of buprenorphine (0.1mg/kg) was used for pain management. The hair on the right leg was removed using Nair® depilatory and sterilized using povidone-iodine swabs. A medial para-patellar incision was made on the right knee and the patella was deflected laterally to expose the trochlear surface. A 1.8mm diameter 1mm deep hole was drilled at the center of the trochlea using the K.1070 High-Speed Rotary Micromotor Kit (Foredom, Bethel, CT) with a 1.8mm trephine (Fine Science Tools, Foster City, CA) to induce an osteochondral defect. Three groups of animals were prepared (N = 18 total, n=6/group) where each group was randomly selected from the total population. The defects were treated with the Bio-Gide® scaffold alone (Group 1), or Bio-Gide® scaffold seeded with primary chondrocytes treated without (Group 2) or with rhAC (Group 3) over a three week period. Only the top, smooth surface of the scaffold was seeded with cells. The inner tissue and skin were than sutured using 4-0 reverse cutting Vicryl sutures (Ethicon) and VetBond® tissue glue (3M, St. Paul, MN). All surgeries were performed in the morning and rats were administered buprenorphine twice a day for 72 hours post-surgery. Animals were housed in pairs for the duration of the time course. At 6 weeks the animals were double euthanized using CO_2 gas and cervical dislocation and the knees were harvested. Samples were fixed in 10% formalin for 24 hours for analysis. The left knees (uninjured) also were harvested as animal-specific internal controls for observation.

Phosphotungstic Acid Hematoxylin Staining and MicroCT Analysis

Fixed samples were stained with phosphotungstic acid hematoxylin (PTAH, Electron Microscopy Sciences, Hatfield, PA) for soft tissue microCT analysis. The soft tissue surrounding the knee was removed and samples were placed in PTAH for 3 days. They were then washed for 3 days in continuous changes of deionized water to remove traces of the stain. MicroCT analysis was performed using the SkyScan 1172 microCT scanner (Bruker, Belgium) at the Temple Medical School Department of Anatomy and Cell Biology. Samples were scanned at a camera resolution of 7.9μm, 0.5 aluminum filter, with a voltage of 80kV, a current of 124μA, a 0.6° rotation step and an 8 frame averaging rate. Raw data were reconstructed using CtRecon and imaged using CtVox (Microphotonics, Allentown, PA) software. Thresholding was performed using CtVox to filter hard/dense tissue as blue and soft tissue as green.

Histological Analysis

Fixed knees were decalcified in Cal-Ex (Thermo Fisher Scientific, Waltham, MA) for 7 days (fresh Cal-Ex was replaced every two days), and then washed for 3 hours in running deionized water followed by washing in 10% formalin for 30 minutes. Samples were serially dehydrated through ethanol/xylene and embedded in paraffin oriented with the medial side of the knee face down. Embedded samples were sectioned at 7μm thickness. Cover slides were rehydrated through xylene/ethanol/water and stained with Harris modified hematoxylin and eosin Y (H&E, Sigma Aldrich, St. Louis, MO) and Toluidine Blue (TB, Sigma Aldrich, St. Louis, MO). Standard protocols for all stains were followed.

Immunohistochemistry

Embedded samples (prepared as above) were immunostained for Collagen II (Col2) and Collagen X (Col10). The Ultravision Detection System (Lab Vision Corporation, Fremont, CA, TR-15-HD) was used to detect the Col2 (Santa Cruz Biotechnology, Dallas, TX, sc-28887) and Col10 (Abcam, Cambridge, UK, ab58632) antibody signals. Briefly, sectioned slides were baked at 65°C for 1 hour, deparaffinized and rehydrated through serial xylene/ethanol gradients to deionized water. 1% proteinase (1:500 dilution) for 15 minutes at 37°C was used for antigen retrieval. Slides were blocked using hydrogen peroxide and the specific kit components, and then incubated in 1° antibody solution containing 5% serum and 0.1% Tween-20 at 4°C overnight (Col2 at 1:500 and Col10 at 1:2500 dilutions). The following day, the slides were brought to room temperature (RT) and incubated in 2° antibody solution for 30 minutes at RT (biotinylated goat anti-rabbit). They were then incubated in streptavidin peroxidase and imaged with DAB chromagen until the tissues turned brown. Hematoxylin was used as a counterstain.

Quantitative Analysis and O'Driscoll Scoring

In order to quantify the quality of the defect healing amongst the different groups, a modified version of the O'Driscoll scoring system was used. Three separate observers scored five different categories from the accepted parameters (matrix staining, surface regularity, structural integrity, cellularity and adjacent cartilage). Each category was scored (n=4 rats for the scaffold only group and n=5 rats each for the cell seeded groups), and

designated 1–4, where 4 indicated the highest quality (i.e., normal healthy cartilage) and 1 was minimal to zero quality. Scoring was performed blinded to the experimental groups. Surface regularity was determined by the smoothness of the surface over the defected area; structural integrity was an observation of the ability of the implanted material to maintain an appropriate environment for tissue integration. Both of these scores were determined using H&E staining. Matrix staining was determined by the presence of Col2 and the absence of Col10 in the chondral region and the presence of Col10 in the subchondral region. Cellularity was a measure regarding the presence of articular-like chondrocytes in the chondral regions of the defected area. Both scores were determined using the immunostained and H&E images. Adjacent cartilage health was determined using the toluidine blue stains and was demonstrated by a higher intensity of GAG content around the periphery of the defected area. Values from each scorer were averaged. Cell treatment (-rhAC and +rhAC) was then compared to scaffold alone to show a relative degree of wound healing. The evaluation was conducted as a blind study, where observers were not aware of treatment groups and scores were tallied afterward.

Statistical Analysis

For the *in vitro* studies depicted in Figure 1, each individual experiment (N=6 for cell number; n=3 each for qRT-PCR and GAG analysis) was performed in triplicate. The means of each independent experiment were presented as a scatter plot and the mean of the total experiments was indicated by a horizontal bar. Vertical bars represent the 95% confidence interval (CI). P values were calculated using unpaired (cell number and GAG content) and paired (qRT-PCR) t-tests. In Figure 2, data was presented similarly to Figure 1; unpaired t-tests were used to determine the P values. For *in vivo* O'Driscoll analysis, images were scored by three independent observers who were blinded to the treatment group; results were compared to healthy cartilage. The mean of the three scores were presented (Table 1) along with the standard deviations and 95% CI. P values were calculated comparing cell treatment (-rhAC or +rhAC) to scaffold alone by a multiple t-test using the *ad hoc* Holm Sidak method for significance with $\alpha = 5.00\%$.

Results

In vitro characterization of rhAC treated chondrocytes

Cells were observed microscopically after 7 days with and without rhAC treatment (Fig. 1A and B), and assessed by qRT-PCR and for GAG content (Fig. 1 D and E). Treatment with rhAC resulted in almost double the number of cells (Fig. 1C), a 3-fold increase in GAG production (Fig. 1D), and also stimulated an increase in the gene expression of specific chondrocyte markers, including ~10-fold increase in Col2, ~4-fold increase in aggrecan and ~5-fold increase in Sox9 (Fig. 1E). rhAC treatment moderately repressed the expression of Col10, a known hypertrophic marker.

Cell-seeding

To evaluate the *in vivo* effects of rhAC treated chondrocytes, Bio-Gide®, a clinically accepted material was used [24]. Bio-Gide® is a biphasic material containing a collagen I top layer and a porous collagen III bottom layer. After 1 week of expansion rhAC treated

and untreated chondrocytes were harvested and seeded at the same cell density onto the Bio-Gide® 3 days prior to implantation (Fig. 2). At 4 and 72 hours an estimated total number of cells on the scaffolds was calculated by counting specific grids after DAPI staining. Of note, at 4 hours more adhered cells could be observed with rhAC treatment. By 72 hours more cells were still evident in the rhAC group, although the differences were smaller.

Osteochondral defect model

To evaluate the rhAC treated chondrocyte-seeded scaffolds *in vivo*, osteochondral defects were generated in 6-month-old Sprague-Dawley rats using a microdrilling procedure (Fig. 3). The dashed circles indicate the injury prior to implantation (left) and after the implant was secured in the defect (right). The animals were housed and observed daily for 6 weeks before euthanasia and tissue analysis, and showed no signs of weight loss or loss of appetite, infection to the wound area or any decreased quality of life. Three independent groups of animals were evaluated (n=6/group): group 1, defect with scaffold but lacking cells; group 2, defect with scaffold and cells that were not treated with rhAC (−rhAC), and group 3, defect with scaffold and rhAC treated cells (+rhAC).

MicroCT evaluation

After the 6 week observation period, macro-scale views gave an indication to the effectiveness of rhAC treated cell-scaffold constructs (Fig. 4). In cell-scaffold implants, areas of what appeared to be an articular-like surface could be observed in all animals, but to a much greater extent in animals receiving rhAC treated cells (Fig. 4G and J, respectively). Fig. S1 depicts additional animals. To clarify the tissue formation in the defected areas, the samples were stained with PTAH and observed with microCT. The micrographs were reconstructed in 3D and threshold adjustments were used to distinguish between soft (green) and hard (blue) tissue. The images revealed little to no appropriate healing in the scaffold alone animals (Fig. 4E and F). The intense green staining in these images represents the collagen-based Bio-Gide® itself. Interestingly, scaffolds seeded with untreated chondrocytes induced tissue formation (Fig. 4H and I), however the new tissue appeared to be more “bone-like” than “cartilage-like”, indicated by the presence of blue growing over the surface of the wound. Scaffolds seeded with rhAC treated chondrocytes (Fig. 4K and L) showed significant improvement in the quality of the newly formed soft tissue (green). Fig. S2 depicts additional animals.

Histological and immunohistochemical assessment

Although the microCT data provided valuable insights into the wound healing mechanism occurring in the different groups, histological staining and immunohistochemistry were used to further validate the findings. Fig. 5 depicts H&E staining. Scaffolds alone induced little to no tissue infiltration into the material, as indicated by the fibrous-like structure seen in the center of the defected area (Fig. 5C) and the fibrous-like scar tissue growing on the surface (Fig. 5D). Scaffolds prepared with cells lacking rhAC treatment revealed enhanced tissue infiltration into the defected area as compared to scaffolds alone, albeit the tissue did not appear to resemble articular cartilage morphology (Fig. 5E and F). In contrast, rhAC treated cell-scaffold constructs yielded what appeared to be an articular-like surface (Fig. 5G), as

well as a more oriented subchondral region in the defect. Higher magnifications revealed a smooth layer on the top of the implant that shares many similarities with articular cartilage, (Fig. 5H). Fig. S3 depicts additional animals.

Further characterization was performed using toluidine blue to visualize GAG content (Fig. 6). With just the scaffold alone very little staining was observed (Fig. 6C and D). However, in animals receiving cell-scaffold implants, GAG accumulation could be observed around the periphery of the defect (Fig. 6E–H), and a thin staining layer also was evident along the surface. The latter was more evident using rhAC treated cells. No observable increase in GAG production was observed within the defected area. Fig. S4 depicts additional animals.

Immunostaining also was used to observe chondrogenic (Col2) and hypertrophic (Col10) tissue formation. Animals implanted with scaffolds alone had little or no Col2 staining present across the surface of the defected area (Fig. 7C). Cell-scaffold implants containing untreated chondrocytes also showed very little Col2 on the surface (Fig. 7E), while rhAC treated cell-scaffold implants showed strong expression of Col2 in the articular-like surface (Fig. 7G). As expected, no Col10 staining was evident on the surface of the defected area in any of the animals (Fig. 7D, F and H). Col10 staining was evident in the subchondral bone of all animals. Fig. S5 depicts additional animals.

We further quantified the histological and immunostaining data using a modified O'Driscoll scoring system, where we observed matrix staining, surface regularity, structural integrity, cellularity and adjacent cartilage. Three independent observers scored the animals and were blinded to the groups. As seen below in Table 1, the addition of rhAC treated cells to the implants led to increases in all categories. Structural integrity was maintained in all three groups, most likely due to having a stable implant in the defected area.

Discussion

The overall goal of this study was to evaluate the utility of rhAC for cell-based cartilage repair using a rat osteochondral defect model. The results confirmed previous *in vitro* findings [8], and documented for the first time positive biochemical and histological outcomes of the implanted cells *in vivo*. In recent years ACI has attracted considerable attention [2,21], however *in vitro* expansion and de-differentiation of chondrocytes prior to implantation limits the utility of this approach [4, 7]. Classical methods to prevent de-differentiation use chondrogenic medium containing TGFβ homologues [3, 25], although other factors have been shown to have similar effects, including BMP2 [5], FGF2 [6] and, recently, rhAC [7]. Researchers have also explored the use of new scaffold materials [26, 27].

In this study chondrocytes were treated with or without rhAC and observed *in vitro* for one week prior to seeding on Bio-Gide® scaffolds. rhAC treatment resulted in more cells, higher GAG content, and increased gene expression of Col2, aggrecan and Sox9 (Fig. 1). How rhAC induces changes in gene expression remains an important question of interest. Previous studies have shown that the lipid substrate of AC, ceramide, has a function in the formation and function of nuclear membranes [28], and that ceramide/S1P crosstalk may

affect gene expression [29, 30]. This suggests that the treatment of chondrocytes with rhAC alters nuclear membrane lipids to induce transcriptional changes, although this remains to be shown.

To test the repair efficiency of the rhAC treated cells, an osteochondral rat defect model was created [22] and a clinically accepted, collagen-based material, Bio-Gide®, was used. Three important *in vitro* characteristics of the cell treatment were observed: a) enhanced cell growth on tissue culture flasks, b) enhanced chondrogenic gene expression and GAG production, and c) enhanced adherence to the Bio-Gide® material.

Post-euthanasia analysis was performed on rats 6 weeks after surgery [31–33]. MicroCT reconstructions were used to visualize the formation of hard/soft tissue at the wound interface, and PTAH was used to stain the soft tissue [34–36]. PTAH acts similarly to iodine in an MRI, and thus was able to distinguish the formation of either hard or soft tissue over the defected area.

It was evident from these analyses that there was soft tissue formation in rats receiving either scaffold alone or cell-scaffold implants. However, it was also clear that scaffold alone induced no real healing, and that much of the soft tissue (green) signal was likely due to the collagen present in the scaffold itself. Moreover, in animals receiving the non-rhAC treated cells there was bony bridge formation along the surface of the implant. Chondrocytes undergo hypertrophy and begin to mineralize ECM during both development and wound healing [37–39]. In animals receiving rhAC treated cell scaffolds microCT analysis revealed a smooth layer of soft tissue over a much more organized subchondral region, which indicated that the scaffold-tissue healing process was much more highly regulated and chondro-specific.

H&E staining further confirmed these findings (Fig. 5). Scaffolds alone and scaffolds containing non-rhAC treated cells yielded fibrous tissue formed around the material and fibrous tissue with a bone-like structure growing across the surface, respectively, while scaffolds containing rhAC treated cells produced an articular-like surface that resembled articular cartilage. The results of toludine blue staining indicated no substantial GAG-rich ECM formation in any of the groups, although animals receiving cell-scaffold implants with rhAC did have a thin layer of strongly stained material along the cell surface (Fig. 6). GAGs are a typical component in the ECM of articular cartilage [32, 33], although it has recently been shown that studies of up to 12 weeks [19] may be required to yield a GAG-rich ECM in implanted materials. Another potential hypothesis for the lack of GAG staining within the implant itself may be that Bio-Gide® inhibits GAG production, although this remains to be proven experimentally.

Importantly, the scaffolds containing rhAC treated cells showed an abundance of Col2 in the ECM of the surface of the implant (Fig. 7). These findings were similar to what was observed *in vitro* (Fig. 1E), where rhAC treatment led to enhanced Col2 expression, and suggested that rhAC had a positive effect on articular cartilage formation *in vivo*. However, to determine whether this is due to the enhanced chondrogenic phenotype of the implanted cells or to the increased number of cells adhered to the scaffolds (Fig. 2) would require

further testing. Both cases, however, are a positive effect of rhAC on chondrocytes and cartilage repair.

Quantification of the histology and immunostains was performed using a modification of the O'Driscoll scoring system, which is typically used to quantify *in vivo* animal studies. The results indicate that the addition of rhAC treated chondrocytes to the scaffold implant yielded better tissue formation and, in particular, cellularity (Table 1). Treatment with rhAC showed smaller rounded cells with a more uniform matrix, indicative of articular cartilage (Fig. 5G – H). Importantly, we have not observed any limitations to the use of rhAC as a media supplement for ACI, although hypothetically it may be possible to "overdose" the cells such that some sphingosine related toxicity is observed, or perhaps to artificially transform the cells due to constitutive overexpression of S1P. These possibilities will be carefully followed in the future.

We propose that this proof-of-concept rodent model provides the appropriate evidence and results to validate future large animal and clinical studies. rhAC is currently being manufactured for the treatment of the rare genetic disorder of AC deficiency, Farber Lipogranulomatosis, and should be available within the next year for evaluation in human clinical trials.

Supplementary Material

Refer to Web version on PubMed Central for supplementary material.

Acknowledgements

The authors would like to acknowledge Dr. Yi Ge for expert technical assistance, Dr. James Iatridis for insightful discussion, and Mamta Amin for technical assistance at Temple University.

Role of funding source

This research was supported by National Institute of Health (NIH) grant R01 DK54830 to EHS.

EHS and CMS are co-inventors on a patent regarding the use of AC for cartilage repair, which has been licensed by the Mount Sinai School of Medicine to Plexcera Therapeutics. EHS is a co-founder and equity holder of Plexcera Therapeutics, receives a research grant and is a consultant to the company. CMS is a consultant to Plexcera Therapeutics.

References

1. CDC. , editor. Control CfD. Osteoarthritis. Center for Disease Control and Prevention; vol. 2013. CDC Website: CDC 2013:Prevelance of Osteoarthritis in the US.
2. Perera JR, Gikas PD, Bentley G. The present state of treatments for articular cartilage defects in the knee. Ann R Coll Surg Engl. 2012; 94:381–387. [PubMed: 22943326]
3. Puetzer JL, Petitte JN, Loboa EG. Comparative Review of Growth Factors for Induction of Three-Dimensional In Vitro Chondrogenesis in Human Mesenchymal Stem Cells Isolated from Bone Marrow and Adipose Tissue. Tissue Engineering Part B-Reviews. 2010; 16:435–444. [PubMed: 20196646]
4. Schulze-Tanzil G. Activation and dedifferentiation of chondrocytes: implications in cartilage injury and repair. Ann Anat. 2009; 191:325–338. [PubMed: 19541465]

5. Ma B, Leijten JC, Wu L, Kip M, van Blitterswijk CA, Post JN, et al. Gene expression profiling of dedifferentiated human articular chondrocytes in monolayer culture. Osteoarthritis Cartilage. 2013; 21:599–603. [PubMed: 23376013]
6. Jakob M, Demarteau O, Schafer D, Hintermann B, Dick W, Heberer M, et al. Specific growth factors during the expansion and redifferentiation of adult human articular chondrocytes enhance chondrogenesis and cartilaginous tissue formation in vitro. J Cell Biochem. 2001; 81:368–377. [PubMed: 11241676]
7. Simonaro CM, Sachot S, Ge Y, He X, Deangelis VA, Eliyahu E, et al. Acid ceramidase maintains the chondrogenic phenotype of expanded primary chondrocytes and improves the chondrogenic differentiation of bone marrow-derived mesenchymal stem cells. PLoS One. 2013; 8:e62715. [PubMed: 23638138]
8. Park JH, Schuchman EH. Acid ceramidase and human disease. Biochim Biophys Acta. 2006; 1758:2133–2138. [PubMed: 17064658]
9. Mao CG, Obeid LM. Ceramidases: regulators of cellular responses mediated by ceramide, sphingosine, and sphingosine-1-phosphate. Biochimica Et Biophysica Acta-Molecular and Cell Biology of Lipids. 2008; 1781:424–434.
10. Van Brocklyn JR, Letterle CA, Snyder PJ, Prior TW. Sphingosine-1-phosphate stimulates human glioma cell proliferation through G(i)-coupled receptors: role of ERK MAP kinase and phosphatidylinositol 3-kinase beta. Cancer Letters. 2002; 181:195–204. [PubMed: 12175535]
11. Masuko K, Murata M, Nakamura H, Yudoh K, Nishioka K, Kato T. Sphingosine-1-phosphate attenuates proteoglycan aggrecan expression via production of prostaglandin E2 from human articular chondrocytes. BMC Musculoskelet Disord. 2007; 8:29. [PubMed: 17374154]
12. Auge N, Nikolova-Karakashian M, Carpentier S, Parthasarathy S, Negre-Salvayre A, Salvayre R, et al. Role of sphingosine 1-phosphate in the mitogenesis induced by oxidized low density lipoprotein in smooth muscle cells via activation of sphingomyelinase, ceramidase, and sphingosine kinase. Journal of Biological Chemistry. 1999; 274:21533–21538. [PubMed: 10419457]
13. Obeid LM, Linardic CM, Karolak LA, Hannun YA. Programmed Cell-Death Induced by Ceramide. Science. 1993; 259:1769–1771. [PubMed: 8456305]
14. Eliyahu E, Park JH, Shtraizent N, He X, Schuchman EH. Acid ceramidase is a novel factor required for early embryo survival. Faseb Journal. 2007; 21:1403–1409. [PubMed: 17264167]
15. Eliyahu E, Shtraizent N, Shalgi R, Schuchman EH. Construction of conditional acid ceramidase knockout mice and in vivo effects on oocyte development and fertility. Cell Physiol Biochem. 2012; 30:735–748. [PubMed: 22854249]
16. Muranjan M, Agarwal S, Lahiri K, Bashyam M. Novel Biochemical Abnormalities and Genotype in Farber Disease. Indian Pediatrics. 2012; 49:320–322. [PubMed: 22565078]
17. Cvitanovic-Sojat L, Juraski RG, Sabourdy F, Fensom AH, Fumic K, Paschke E, et al. Farber lipogranulomatosis type 1-Late presentation and early death in a Croatian boy with a novel homozygous ASAH1 mutation. European Journal of Paediatric Neurology. 2011; 15:171–173. [PubMed: 20609603]
18. Ramsubir S, Nonaka T, Girbes CB, Carpentier S, Levade T, Medin JA. In vivo delivery of human acid ceramidase via cord blood transplantation and direct injection of lentivirus as novel treatment approaches for Farber disease. Molecular Genetics and Metabolism. 2008; 95:133–141. [PubMed: 18805722]
19. Dahlin RL, Kinard LA, Lam J, Needham CJ, Lu S, Kasper FK, et al. Articular chondrocytes and mesenchymal stem cells seeded on biodegradable scaffolds for the repair of cartilage in a rat osteochondral defect model. Biomaterials. 2014; 35:7460–7469. [PubMed: 24927682]
20. Chung JY, Song M, Ha CW, Kim JA, Lee CH, Park YB. Comparison of articular cartilage repair with different hydrogel-human umbilical cord blood-derived mesenchymal stem cell composites in a rat model. Stem Cell Res Ther. 2014; 5:39. [PubMed: 24646697]
21. Hui JH, Goyal D, Nakamura N, Ochi M. Cartilage repair: 2013 Asian update. Arthroscopy. 2013; 29:1992–2000. [PubMed: 24286798]
22. Chu CR, Szczodry M, Bruno S. Animal models for cartilage regeneration and repair. Tissue Eng Part B Rev. 2010; 16:105–115. [PubMed: 19831641]

23. He X, Okino N, Dhami R, Dagan A, Gatt S, Schulze H, et al. Purification and characterization of recombinant, human acid ceramidase. Catalytic reactions and interactions with acid sphingomyelinase. J Biol Chem. 2003; 278:32978–32986. [PubMed: 12815059]
24. Gomoll AH, Probst C, Farr J, Cole BJ, Minas T. Use of a Type I/III Bilayer Collagen Membrane Decreases Reoperation Rates for Symptomatic Hypertrophy After Autologous Chondrocyte Implantation. American Journal of Sports Medicine. 2009; 37:20s–23s. [PubMed: 19841142]
25. Studer D, Millan C, Ozturk E, Maniura-Weber K, Zenobi-Wong M. Molecular and Biophysical Mechanisms Regulating Hypertrophic Differentiation in Chondrocytes and Mesenchymal Stem Cells. European Cells & Materials. 2012; 24:118–135. [PubMed: 22828990]
26. Torricelli P, Gioffre M, Fiorani A, Panzavolta S, Gualandi C, Fini M, et al. Co-electrospun gelatin-poly(l-lactic acid) scaffolds: Modulation of mechanical properties and chondrocyte response as a function of composition. Mater Sci Eng C Mater Biol Appl. 2014; 36:130–138. [PubMed: 24433895]
27. Li C, Zhang J, Li Y, Moran S, Khang G, Ge Z. Poly (l-lactide-co-caprolactone) scaffolds enhanced with poly (beta-hydroxybutyrate-co-beta-hydroxyvalerate) microspheres for cartilage regeneration. Biomed Mater. 2013; 8:025005. [PubMed: 23385654]
28. Shiraishi T, Imai S, Uda Y. The presence of ceramidase activity in liver nuclear membrane. Biol Pharm Bull. 2003; 26:775–779. [PubMed: 12808285]
29. Beckham TH, Lu P, Cheng JC, Zhao D, Turner LS, Zhang X, et al. Acid ceramidase-mediated production of sphingosine 1-phosphate promotes prostate cancer invasion through upregulation of cathepsin B. Int J Cancer. 2012; 131:2034–2043. [PubMed: 22322590]
30. Beckham TH, Cheng JC, Lu P, Marrison ST, Norris JS, Liu X. Acid ceramidase promotes nuclear export of PTEN through sphingosine 1-phosphate mediated Akt signaling. PLoS One. 2013; 8:e76593. [PubMed: 24098536]
31. Ferretti M, Marra KG, Kobayashi K, Defail AJ, Chu CR. Controlled in vivo degradation of genipin crosslinked polyethylene glycol hydrogels within osteochondral defects. Tissue Engineering. 2006; 12:2657–2663. [PubMed: 16995799]
32. Unterman SA, Gibson M, Lee JH, Crist J, Chansakul T, Yang EC, et al. Hyaluronic Acid-Binding Scaffold for Articular Cartilage Repair. Tissue Engineering Part A. 2012; 18:2497–2506. [PubMed: 22724901]
33. Needham CJ, Shah SR, Dahlin RL, Kinard LA, Lam J, Watson BM, et al. Osteochondral tissue regeneration through polymeric delivery of DNA encoding for the SOX trio and RUNX2. Acta Biomaterialia. 2014; 10:4103–4112. [PubMed: 24854956]
34. Buytaert J, Goyens J, De Greef D, Aerts P, Dirckx J. Volume Shrinkage of Bone, Brain and Muscle Tissue in Sample Preparation for Micro-CT and Light Sheet Fluorescence Microscopy (LSFM). Microsc Microanal. 2014; 20:1208–1217. [PubMed: 24963987]
35. Dunmore-Buyze PJ, Tate E, Xiang FL, Detombe SA, Nong Z, Pickering JG, et al. Three-dimensional imaging of the mouse heart and vasculature using micro-CT and whole-body perfusion of iodine or phosphotungstic acid. Contrast Media Mol Imaging. 2014; 9:383–390. [PubMed: 24764151]
36. Das Neves Borges P, Forte AE, Vincent TL, Dini D, Marenzana M. Rapid, automated imaging of mouse articular cartilage by microCT for early detection of osteoarthritis and finite element modelling of joint mechanics. Osteoarthritis Cartilage. 2014; 22:1419–1428. [PubMed: 25278053]
37. Zhou X, von der Mark K, Henry S, Norton W, Adams H, de Crombrugghe B. Chondrocytes Transdifferentiate into Osteoblasts in Endochondral Bone during Development, Postnatal Growth and Fracture Healing in Mice. PLoS Genet. 2014; 10:e1004820. [PubMed: 25474590]
38. Sheehy EJ, Vinardell T, Toner ME, Buckley CT, Kelly DJ. Altering the architecture of tissue engineered hypertrophic cartilaginous grafts facilitates vascularisation and accelerates mineralisation. PLoS One. 2014; 9:e90716. [PubMed: 24595316]
39. Bahney CS, Hu DP, Taylor AJ, Ferro F, Britz HM, Hallgrimsson B, et al. Stem cell-derived endochondral cartilage stimulates bone healing by tissue transformation. J Bone Miner Res. 2014; 29:1269–1282. [PubMed: 24259230]

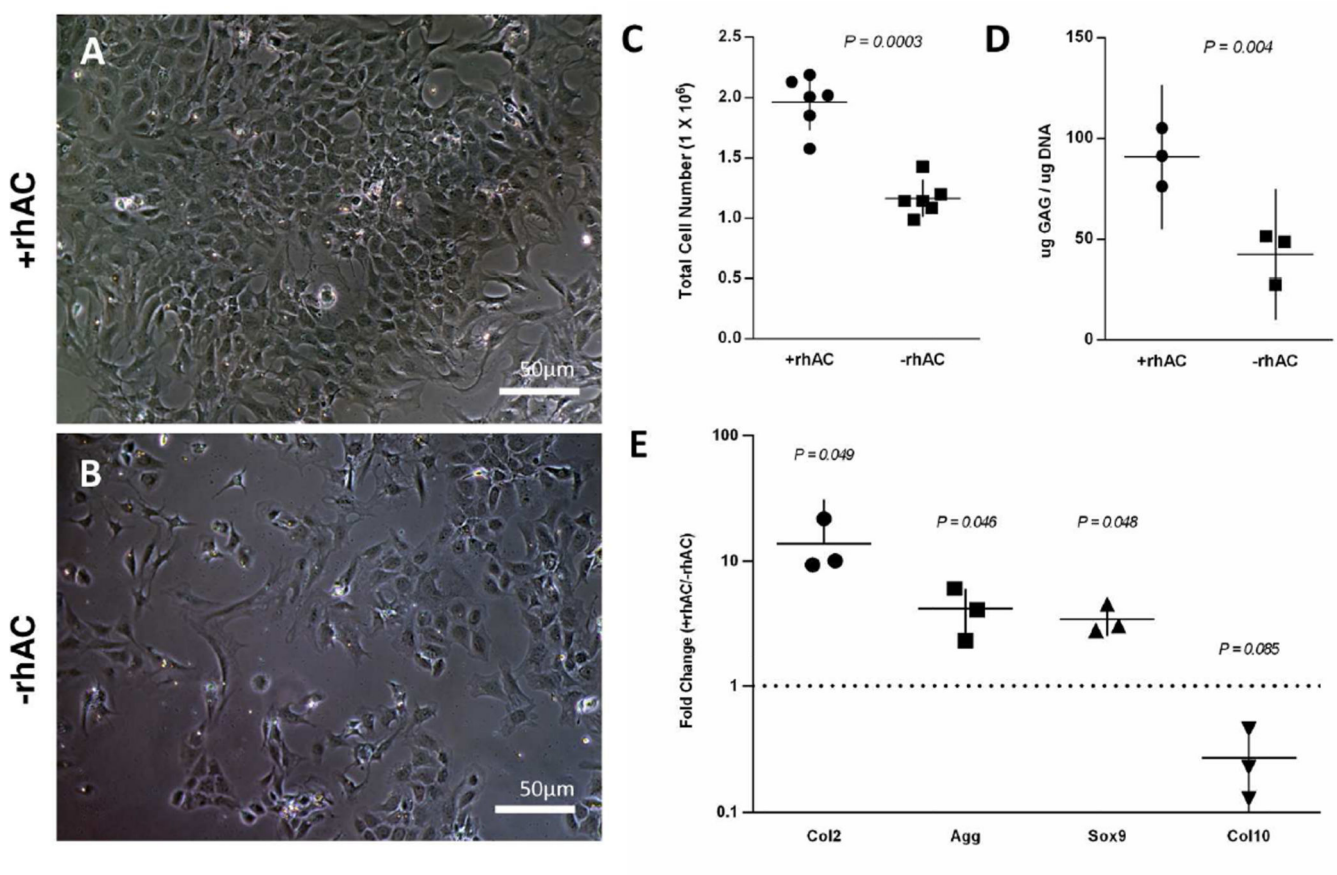

Figure 1.

Primary rat chondrocytes cultured with (A) and without (B) rhAC treatment. The graphs to the right indicate the total cell number (C), GAG content (D), and the relative fold changes in gene expression of Col2, Agg, Sox9 and Col10 as determined by RT-qPCR (E) at day 7. Horizontal lines indicate the mean of individual experiments, and vertical bars indicate the 95% CI. P values were calculated using unpaired (C and D) and paired (E) t-tests. N = 6 experiments (cell number) and n = 3 experiments (GAG content and RT-qPCR). The dotted line in (E) indicates equal expression with and without rhAC treatment. P values compare fold change of rhAC treated versus non-treated cells.

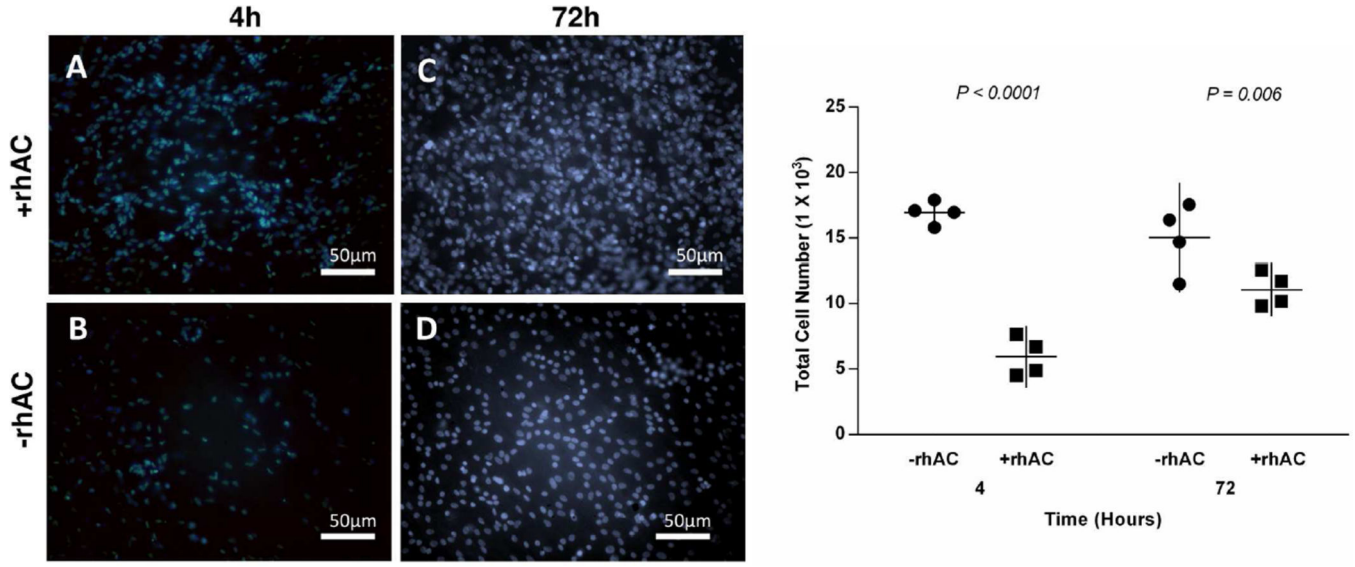

Figure 2.

Bio-Gide® scaffolds seeded with primary rat chondrocytes treated with (A and C) and without (B and D) rhAC. The nuclear stain DAPI (Blue) was used to visualize cells on the scaffolds at 4 and 72 hours after seeding. Cell number was counted and compared using ImageJ. Means from the independent experiments (N = 4 per group) are indicated by the horizontal lines, and the 95% CI is shown as the vertical lines. P values were calculated using unpaired t-tests.

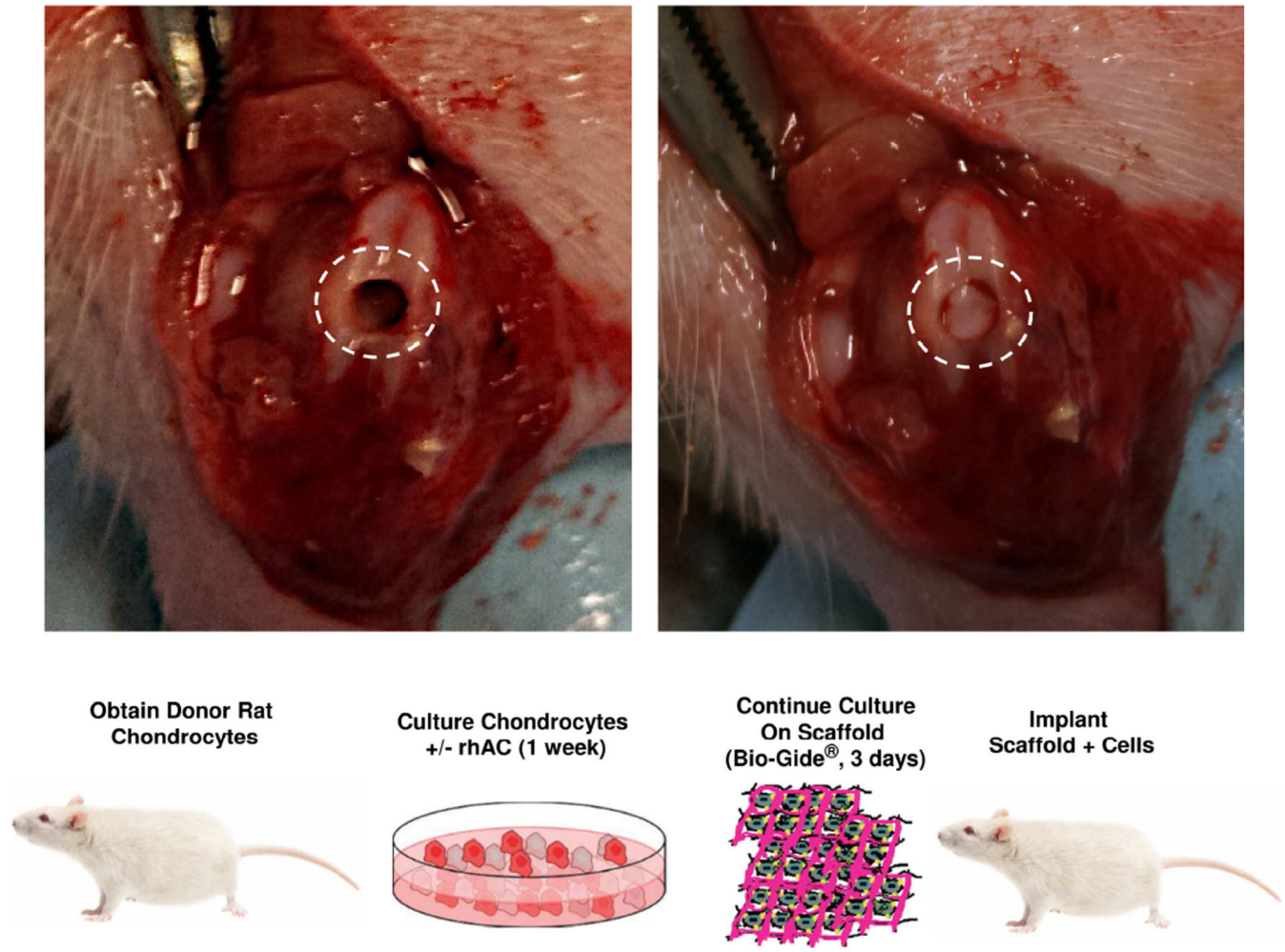

Figure 3.

A representation of the treated protocol used in the osteochondral defect rat model. This tissue engineering based approach utilized a clinically approved matrix (Bio-Gide®) and compared the effects of scaffolds alone to scaffolds seeded with cells +/− rhAC treatment. The images on the top show the osteochondral defect prior to implantation (left), and after implantation (right) with Bio-Gide®.

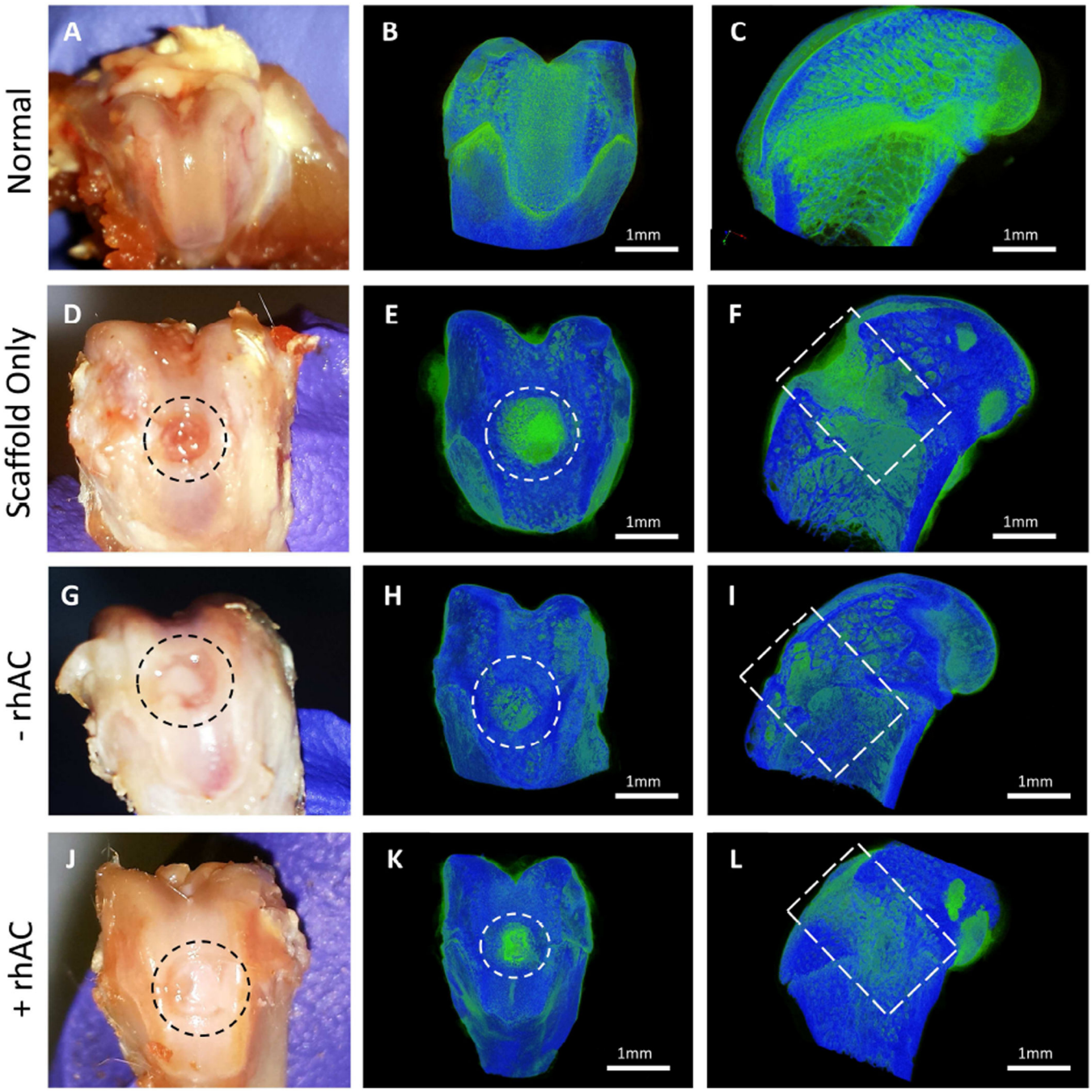

Figure 4.

Gross macroscopic view and microCT imaging of treated osteochondral defects 6-weeks post-surgery. Normal tissues presented for comparison to treatment groups (A–C). Representative images for scaffold alone (D – F), −rhAC scaffolds (G – I) and +rhAC scaffolds (J – L) are presented to show the effects on wound healing with implantation. The regions of interest are shown inside the dotted circles. Scale bars on MicroCT images = 1mm. Images are representative of n=6 samples.

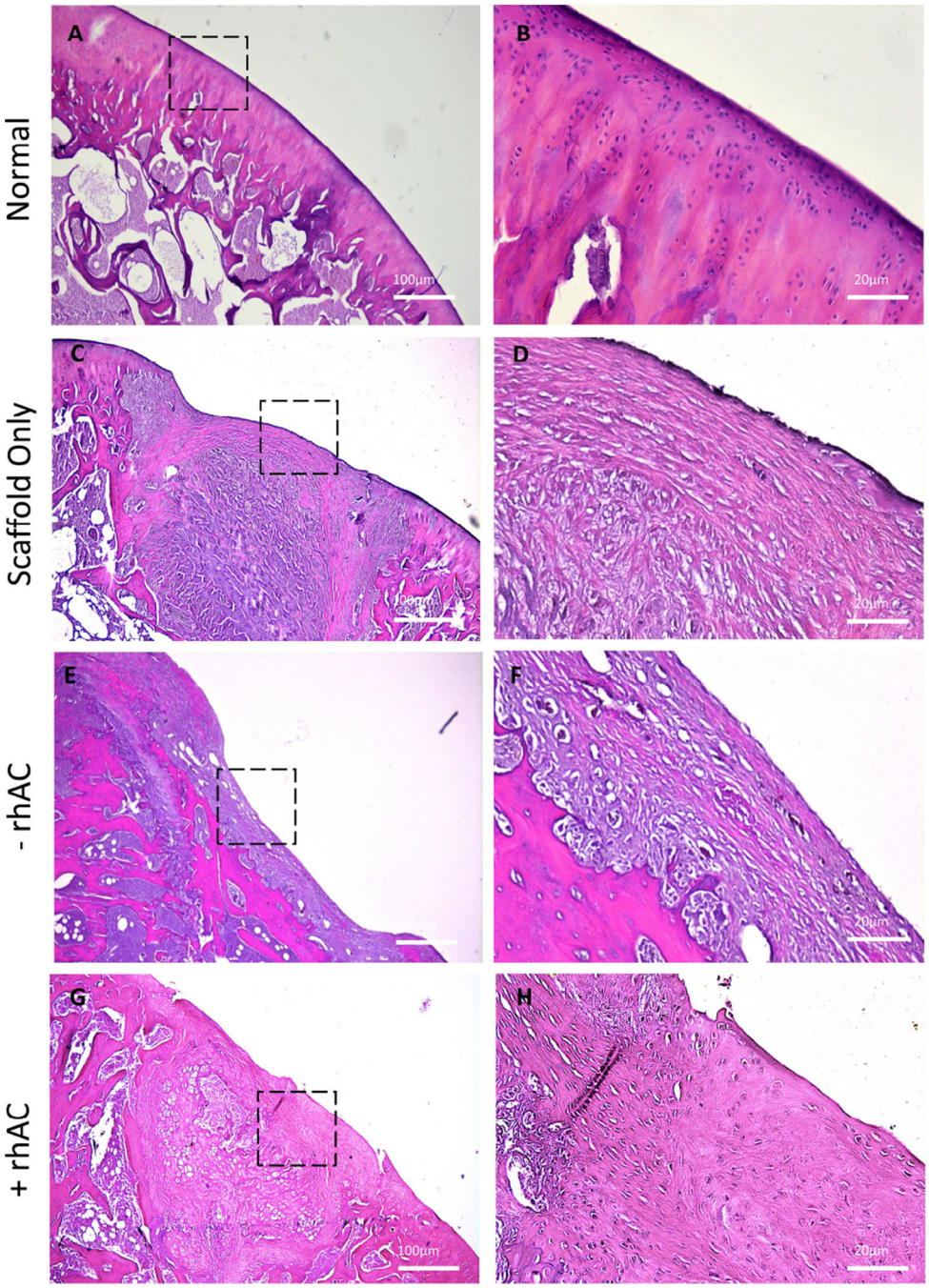

Figure 5.

H&E staining of normal cartilage (A and B), implants containing Bio-Gide® alone (C and D), chondrocytes without rhAC treatment (E and F), and chondrocytes with rhAC treatment (G and H). Dotted boxes represent the region from 4× that is depicted at 20×. Small, rounded chondrocyte-like cells also were evident in scaffolds with rhAC treated cells (H, arrow). Scale bars = 100μm for 4× magnification (A, C, E and G) and 20μm for 20× magnification (B, D, F and H).

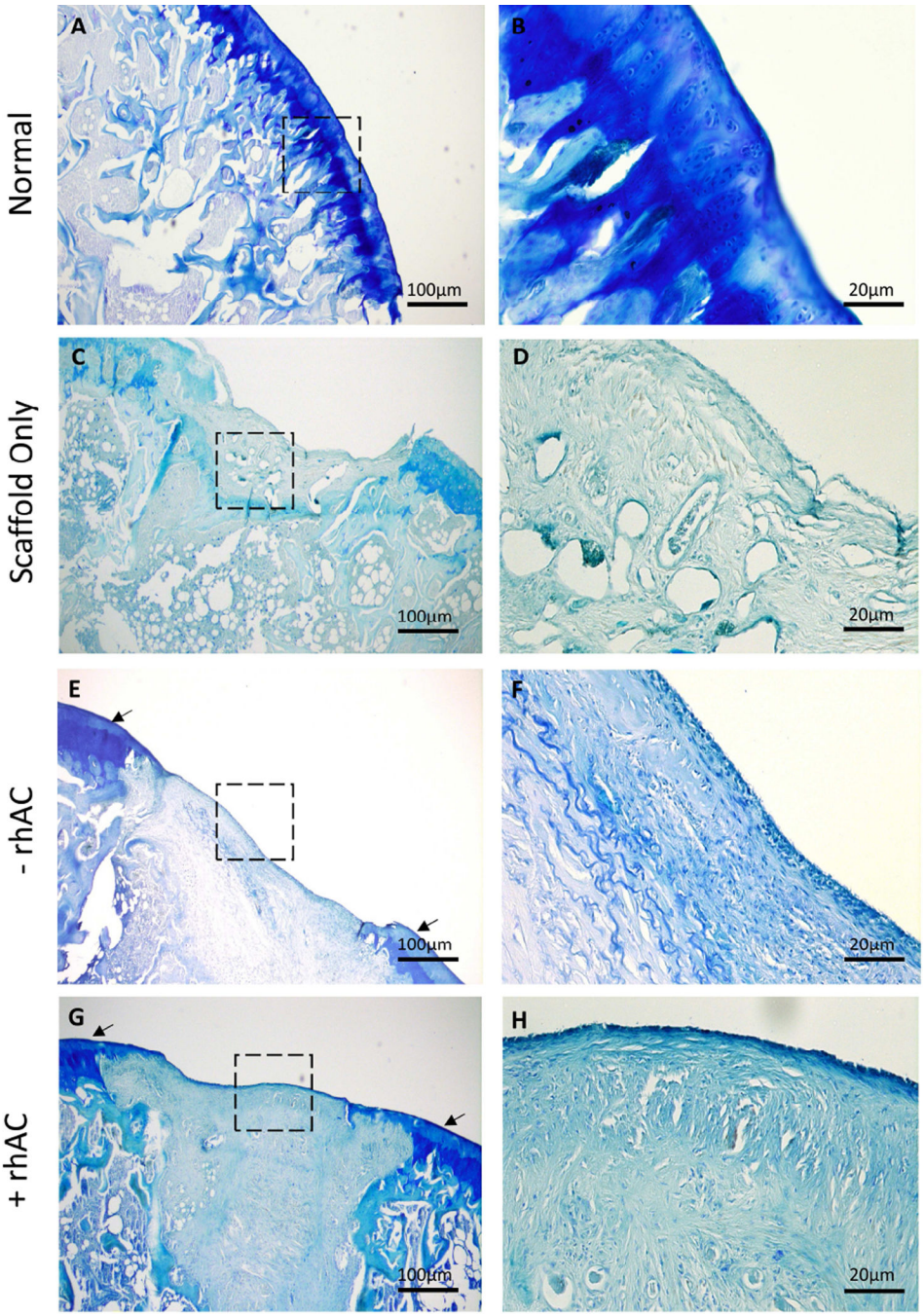

Figure 6.

Toluidine Blue stains of normal cartilage (A and B) Bio-Gide® alone (C and D), Bio-Gide® containing chondrocytes without rhAC treatment (E and F) and chondrocytes with rhAC treatment (G and H). Dotted boxes represent the region from 4× that is depicted at 20×. Arrows indicate strong straining at the periphery of the defected area. Scale bars = 100μm for 4× magnification (A, C, E and G) and 20μm for 20× magnification (B, D, F and H).

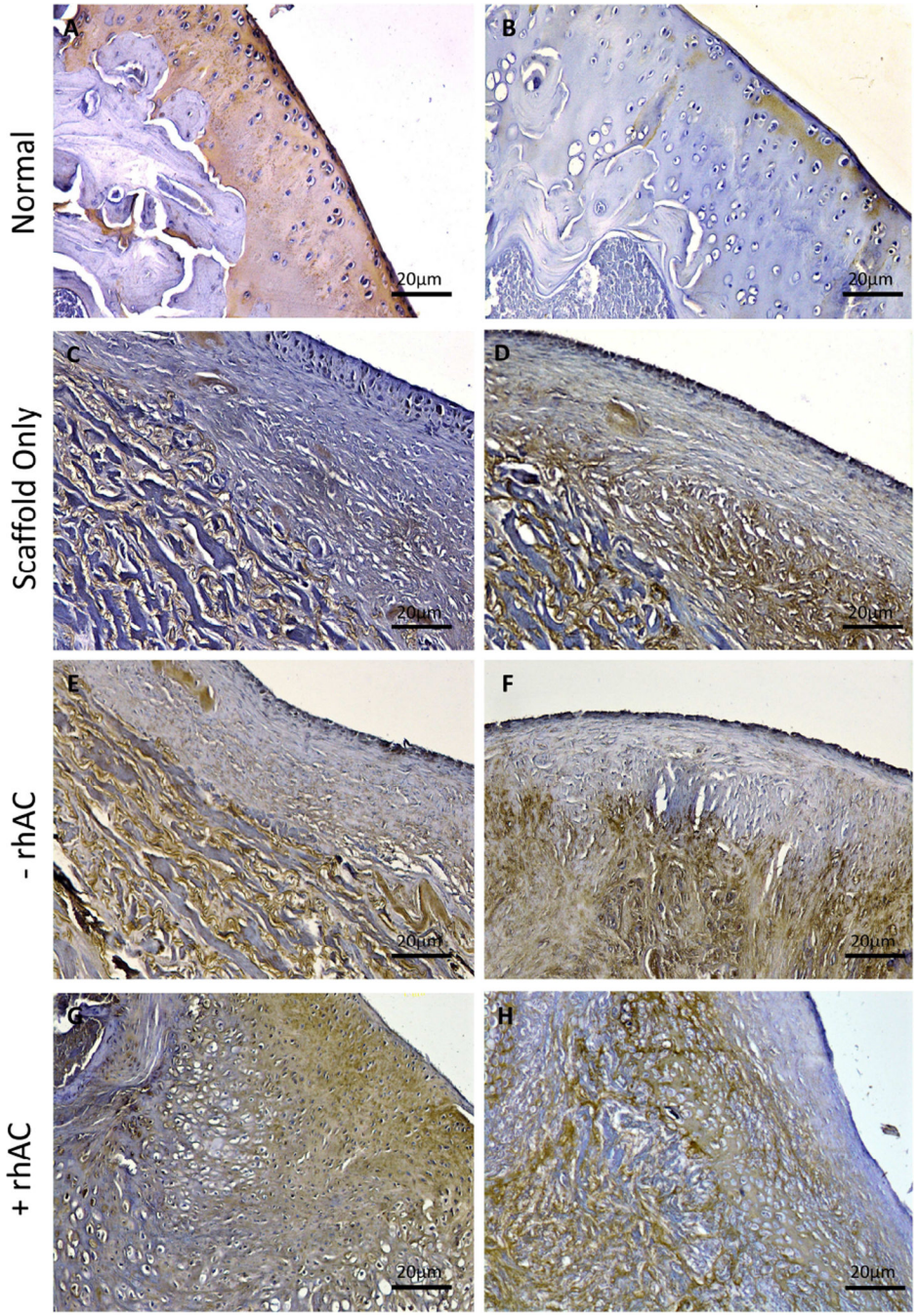

Figure 7.

Col2 and Col10 immunostaining of Bio-Gide® implants. Representative images of normal cartilage (A and B), implants containing Bio-Gide® alone (C and D), chondrocytes without rhAC treatment (E and F), and chondrocytes with rhAC treatment (G and H). Dotted boxes represent the region from 4× that is depicted at 20×. Scale bars = 20μm for 20× magnification.

Table I

Modified O'Driscoll scoring system for quantitative analysis of wound healing.

Scoring (1–4)	Matrix Staining	P	Surface Regularity	P	Structural Integrity	P	Cellularity	P	Adjacent Cartilage	P
Scaffold	1.3 ± 0.5		1.8 ± 0.1		3.8 ± 0.5		1.0 ± 0.0		1.2 ± 0.5	
−rhAC	1.4 ± 0.6 (−0.1 – 0.7)	*0.68*	1.6 ± 0.9 (−1.3 – 1.6)	*0.82*	3.8 ± 0.4 (−0.8 – 0.7)	*0.88*	1.4 ± 0.6 (−1.1 – 0.3)	*0.19*	2.2 ± 1.3 (−2.6 – 0.7)	*0.21*
+rhAC	3.2 ± 1.3 (−3.6 – −0.3)	*0.03*	3.2 ± 0.8 (−2.9 – −0.1)	*0.04*	4.0 ± 0.0 (−0.7 – 0.2)	*0.29*	3.2 ± 0.8 (−3.2 – −1.2)	*0.001*	2.6 ± 1.3 (−3.0 – 0.3)	*0.10*

Data presented as scoring average of 3 independent scorers ± standard deviation (95% CI). P values compare cell treated scaffolds (−rhAC or + rhAC) to scaffold alone.